Journal of Power Sources 195 (2010) 3645–3648

Contents lists available at ScienceDirect

Journal of Power Sources

journal homepage: www.elsevier.com/locate/jpowsour

Short communication

Detailed investigation of ion exchange in ball-milled LiH + MgB_2 system using ultra-high field nuclear magnetic resonance spectroscopy

Jian Zhi Hu [a,*], Ja Hun Kwak [a], Zhenguo Yang [a], Xuefei Wan [b], Leon L. Shaw [b,**]

[a] Pacific Northwest National Laboratory, Richland, WA 99352, USA
[b] Department of Chemical, Materials and Biomolecular Engineering, University of Connecticut, 97 Eagleville Road, Storrs, CT 06269, USA

ARTICLE INFO

Article history:
Received 9 November 2009
Received in revised form 7 December 2009
Accepted 8 December 2009
Available online 16 December 2009

Keywords:
Hydrogen storage
Lithium borohydride
Magnesium diboride
^{6}Li nuclear magnetic resonance

ABSTRACT

The present study with the detailed ^{1}H–^{6}Li cross polarization NMR analysis confirms the formation of a ternary compound, $(Mg_{1-x}Li_{2x})B_2$, during ball milling of LiH + (1/2)MgB_2 at room temperature. The ^{6}Li sites in $(Mg_{1-x}Li_{2x})B_2$ exhibit spinning sidebands (SSBs), whereas the ^{6}Li sites in LiH do not. The SSBs and the very short spin-lattice relaxation time manifested by the ^{6}Li sites in $(Mg_{1-x}Li_{2x})B_2$ indicate that the Li ions in $(Mg_{1-x}Li_{2x})B_2$ are located between the layered boron structures and close to Mg ions. The formation of $(Mg_{1-x}Li_{2x})B_2$ explains the previous observation that the LiH + (1/2)MgB_2 mixture ball-milled effectively has a greatly enhanced hydriding kinetics at temperatures below the melting point of $LiBH_4$.

1. Introduction

The hydrogen storage materials based on $LiBH_4 + MgH_2$ mixtures have the potential for reversible on-board hydrogen storage applications because the following reaction has been shown to have a favorable dehydrogenation enthalpy ($\Delta H = \sim 44$ kJ mol^{-1}) [1]:

$$LiBH_4 + (1/2)MgH_2 = LiH + (1/2)MgB_2 + 2H_2 \quad (1)$$

Reaction (1) also possesses a theoretical storage capacity of 11.5 wt.%. In spite of its favorable thermodynamic properties and high theoretical storage capacity, the kinetics of Reaction (1) is very sluggish. As a result, hydriding and dehydriding of $LiBH_4 + MgH_2$ systems are normally carried out at temperatures above the melting point of $LiBH_4$ (~280 °C) [1–6]. Recently, by combining nanoengineering and mechanical activation achieved through high-energy ball milling, Wan et al. [7] have demonstrated hydriding and dehydriding of LiH + (1/2)MgB_2 mixtures at 265 °C with a hydrogen uptake of 8.3 wt.%. The dramatic improvement in the hydrogen uptake kinetics below the melting point of $LiBH_4$ has been attributed to a Li–Mg ion exchange mechanism taken place during high-energy ball milling [8]. This Li–Mg ion exchange mechanism leads to the formation of a ternary compound with a composition of $(Mg_{1-x}Li_{2x})B_2$ where x is a variable changing from 0 to less than 1. The formation of $(Mg_{1-x}Li_{2x})B_2$ is expected to facilitate the formation of $LiBH_4$ in the subsequent hydriding reaction because the formation of $LiBH_4$ requires the removal of Mg ions from MgB_2 in conjunction of the simultaneous insertion of Li and H ions.

In the previous study [8] the formation of $(Mg_{1-x}Li_{2x})B_2$ is identified by examining ^{6}Li, ^{11}B, and ^{25}Mg nuclear magnetic resonance (NMR) spectra of ball-milled LiH + (1/2)MgB_2 mixtures using the approach of the single pulse (SP) sequence. Given the significance of this ion exchange mechanism as a guideline for designing $LiBH_4 + MgH_2$ storage systems in the future, further investigation using ^{1}H–^{6}Li cross polarization (CP) was performed in this study. The results of this study confirm that the Li–Mg ion exchange mechanism proposed in the previous study [8] is correct; however, this study also reveals that there are errors in the previous assignment of ^{6}Li magic angle spinning (MAS) peaks. The detailed findings of this study are reported below.

2. Materials and methods

Lithium hydride (LiH) of 95% purity and magnesium diboride (MgB_2) of ~98% purity were purchased from Alfa Aesar and used without any pretreatment. The LiH and MgB_2 mixture was prepared with a molar ratio of 1:1/2 according to reaction (1). The high-energy ball milling of the LiH + (1/2)MgB_2 mixture was performed using a modified Szegvari attritor which is effective in preventing the formation of the dead zone and producing uniform milling products within the powder charge [9]. The canister of the attritor and the balls (6.4 mm in diameter) were made of a stainless steel. The loading of the powder mixture and the

* Corresponding author.
** Corresponding author. Leon.Shaw@uconn.edu (L.L. Shaw) Tel.: +1 860 486 2592; fax: +1 860 486 4745.
E-mail addresses: Jianzhi.Hu@pnl.gov (J.Z. Hu),.

0378-7753/$ – see front matter © 2009 Elsevier B.V. All rights reserved.
doi:10.1016/j.jpowsour.2009.12.033

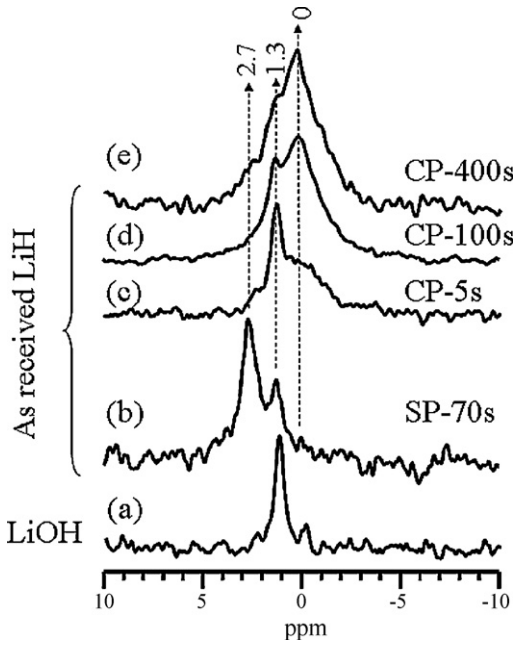

Fig. 1. ^{6}Li MAS spectra. (a) LiOH, acquired using a sample spinning rate of 19 kHz and SP sequence with a recycle delay time of 1024 s and an accumulation number of 49. (b) LiH, acquired using a sample spinning rate of 10 kHz and SP sequence with a recycle delay time of 70 s and an accumulation number of 64. (c–e) LiH, acquired using ^{1}H–^{6}Li CP with a contact time of 2 ms, and a recycle delay time/accumulation number of scans: (c) 5 s/4096, (d) 100 s/426, and (e) 400 s/4, respectively. High power ^{1}H decoupling was applied in (b)–(e).

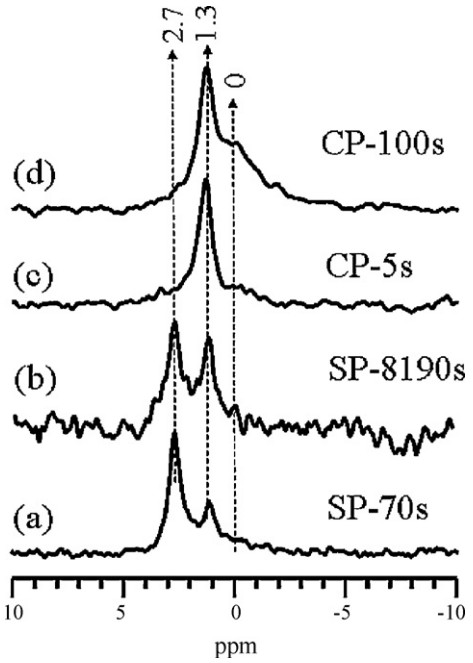

Fig. 2. ^{6}Li MAS spectra of 45 min ball-milled LiH. (a) and (b) were acquired using a SP sequence with high power ^{1}H decoupling with a recycle delay time/accumulation of scans of (a) 70 s/64 and (b) 8192 s/3. (c) and (d) were acquired using ^{1}H–^{6}Li CP sequence with a contact time of 2 ms and a recycle delay time/accumulation number of scans of (c) 5 s/4096 and (d) 100 s/638.

balls to the canister was performed in a glove-box filled with ultra-high-purity argon, the composition of which in the gas tank is Ar 99.999%, N_2 < 5 ppm, H_2 < 3 ppm, H_2O < 1 ppm, O_2 < 1 ppm, and THC < 0.5 ppm. The ball-to-powder weight ratio was 60:1, the milling speed was 600 rpm, the milling atmosphere was ultra-high-purity argon, and the milling temperature was maintained at 20 °C, achieved by water cooling at a flowing rate of 770 ml min^{-1}. Ball milling time was 24 h. Pure LiH was also ball-milled using the same milling conditions except a shorter milling time (i.e., 45 min).

The LiH and LiH + (1/2)MgB_2 mixtures before and after ball milling were analyzed using ^{6}Li single pulse (SP) MAS and ^{1}H–^{6}Li cross polarization (CP) MAS NMR spectroscopy at ultra-high magnetic field of 21.1 T. The corresponding Lamor frequencies for ^{1}H and ^{6}Li were 900.602 and 132.531 MHz, respectively. All the samples were stored in a dry argon glove-box and loaded into sealed NMR rotors while inside the glove-box. Each sample rotor was further protected by placing it inside a sealed glass bottle prior to transferring the sample rotor to the MAS probe. Immediately after loading the sample rotor into the MAS probe, the sample was spun to the targeted sample spinning rate using dry N_2 as both the driving and the bearing gas. In this way oxidation during NMR analysis is minimized. A home-made 3.2 mm pencil type MAS probe was used for all the NMR experiments. About 5–8 mg of samples was used for each measurement. The spectra were referenced to 1 M LiCl (0 ppm) using solid LiCl (−1.25 ppm) as a secondary reference due to its sharp MAS line width at 21.1 T field, i.e., about 15 Hz. To assist the identification of the NMR peaks, lithium hydroxide (LiOH) of >98% purity was purchased from Aldrich and used directly in the NMR analysis.

3. Results and discussion

Fig. 1(a) shows the ^{6}Li MAS spectrum of the as-purchased LiOH. It is found that the ^{6}Li spin-lattice relaxation time in LiOH is very long (>1024 s). Using a recycle time of 64 s, no signal is observed due to signal saturation. Thus, a recycle time of 1024 s is used to acquire the spectrum in Fig. 1(a). A dominant peak located at ∼1.3 ppm is observed and assigned to bulk LiOH. The ^{6}Li MAS spectrum of the as-received LiH acquired using a recycle delay time of 70 s is shown in Fig. 1(b), where two peaks are observed with one at 2.78 ppm and the other at 1.3 ppm. To clarify the chemical identities of these two peaks, ^{1}H–^{6}Li CP experiments at various recycle delay times have been conducted. The results are summarized in Fig. 1(c)–(e). Since in a CP experiment only the ^{6}Li sites that are dipolar-coupled to ^{1}H will generate a signal, this technique can differentiate the Li sites that are close to ^{1}H from those that are not. With a recycle delay time of 5 s (Fig. 1(c)), the spectrum is dominated by a 1.3 ppm peak accompanied by a broad peak centered at about 0 ppm. With increasing the recycle delay time (Fig. 1(d) and (e)), the relative contribution of the 0 ppm peak is significantly increased. Since the peak located at 2.78 ppm does not appear in a CP experiment, the 2.7 ppm peak is assigned to Li_2O based on the same 2.78 ppm peak obtained on the standard Li_2O sample [10]. The 1.3 ppm peak in the CP experiment is assigned to LiOH because there are ^{1}H (protons) close to these Li sites. This assignment is also consistent with Fig. 1(a) of the standard LiOH spectrum. The 0 ppm peak in the CP experiment can thus be safely assigned to bulk LiH. The reason that a very long recycle time, more than 100 s, is needed in a CP experiment to polarize the protons is because the protons in bulk LiH relaxes much slower (hence a much longer T_1) than that in LiOH.

The effect of 45 min of ball milling on LiH is summarized in Fig. 2. Similar to the as-received LiH (Fig. 1(b)), at a recycle delay time of 70 s two peaks, 2.78 ppm (Li_2O) and 1.3 ppm (LiOH), are observed for the 45 min milled LiH (Fig. 2(a)). However, the signal-to-noise ratio is apparently higher in Fig. 2(a) than that in Fig. 1(b) given the same number of scans, 64. This indicates that the corresponding ^{6}Li T_1 in the ball-milled sample is shorter than that in the as-received LiH. The improved signal-to-noise ratio can be attributed to the reduced particle sizes induced by ball milling. When the recycle delay time in the SP experiment increases to 8192 s (Fig. 2(b)), the relative contribution of LiOH peak increases significantly and the

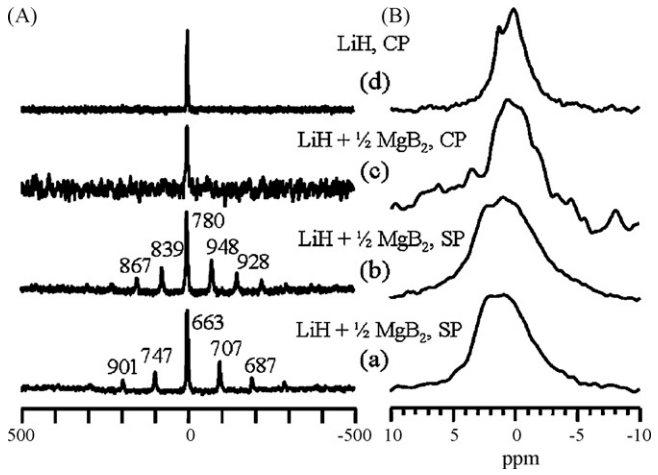

Fig. 3. ^{6}Li MAS spectra. Panel (A) gives the full spectral width, while Panel (B) highlights the corresponding centerband spectra between the chemical shift ranges from −10 to 10 ppm. (a), (b) and (c) were obtained on the 24 h ball-milled LiH + (1/2)MgB_2 sample, whereas (d) was obtained on the as-received LiH. The experimental details are as follows. (a) and (b) were acquired using single pulse with high power ^{1}H decoupling, and the recycle delay time and the total number of accumulation numbers are (a) 0.2 s/4000 and (b) 70 s/188. (c) was acquired using the CP sequence with a contact time of 2 ms, recycle delay time of 1 s and 30,000 accumulations. (d) The CP spectrum of the as-received LiH acquired using a contact time of 2 s and a recycle delay time of 100 s and 426 accumulations. (a) was acquired at a sample spinning rate of 12.5 kHz, while (b), (c) and (d) were acquired at a 9 kHz spinning rate. The numbers labeled by the spinning sideband in (a) and (b) are the half linewidth of the corresponding sideband peak.

LiH peak at 0 ppm becomes visible. These results indicate that the ^{6}Li sites inside LiH have the longest relaxation time, whereas the ^{6}Li sites inside Li_2O have the shortest relaxation time with the relaxation time of the ^{6}Li sites inside LiOH between these two extremes. This is consistent with the conclusion derived from Fig. 1.

Compared with the CP spectra acquired on the as-received LiH with a recycle delay time of 5 s (Fig. 1(c)) and 100 s (Fig. 1(d)), the relative peak intensities of the LiH peak (0 ppm) in the 45 min milled LiH (Fig. 2(c) and (d)) are significantly lower, or the relative peak intensity for the LiOH peak (1.3 ppm) is significantly increased. One possible reason for this is the oxidation of LiH during ball milling. Another possible reason is that the enhancement in LiOH and Li_2O peak intensities induced by ball milling is larger than that in the LiH peak intensity because LiOH and Li_2O are on the surface of LiH particles. Being on the surface of LiH particles, LiOH and Li_2O will experience more deformation and more defects will be introduced to them during ball milling. As such, their relaxation times will be shortened more than that of the ^{6}Li sites inside LiH. We believe that the second possibility is more likely because a previous study [11] under the same ball milling condition has clearly established no oxidation during ball milling of LiH. The significantly enhanced hydrogenation of the ball-milled LiH + (1/2)MgB_2 [7] also supports that no oxidation takes place during ball milling of LiH.

Fig. 3 shows the ^{6}Li MAS spectra of the 24 h ball-milled LiH + (1/2)MgB_2 mixture. It is apparent from Fig. 3(a) and (b) that sample spinning sidebands (SSBs) with significant intensities relative to the centerband are observed at a sample spinning rate of around 10 kHz (12.5 kHz for Fig. 3(a) and 9 kHz for Fig. 3(b)). The half linewidth, defined as the linewidth at the half height positions of the peak, of the centerband is less than those of the SSBs in both Fig. 3(a) and (b), indicating that part of the centerband signal does not produce SSBs. In addition, there is no SSB observed in the SP experiments of the as-received LiH and the 45 min milled LiH sample (not shown here). Furthermore, there was no SSB observed in the CP spectra of the 24 h ball-milled LiH + (1/2)MgB_2 sample (Fig. 3(c)) and the as-received LiH (Fig. 3(d)). Given the fact that CP only detects Li sites that are close to protons, Fig. 3(d) indicates that bulk LiH does not generate SSBs at sample spinning rate of above ~9 kHz. For the 24 h ball-milled LiH + (1/2)MgB_2 sample, the CP experiment (Fig. 3(c)) only probes the ^{6}Li sites within bulk LiH and shows no SSBs. In contrast, the SP experiments (Fig. 3(a) and (b)) detect all ^{6}Li sites and show SSBs. Since the ^{6}Li sites within bulk LiH do not exhibit SSBs, the observed SSBs must come from the Li ions dissolved in MgB_2. In other words, the ternary compound, $(Mg_{1-x}Li_{2x})B_2$, is formed during ball milling of LiH + (1/2)MgB_2. The Li ions in $(Mg_{1-x}Li_{2x})B_2$ will not contribute to the CP spectrum of Fig. 3(c) because there is no proton in $(Mg_{1-x}Li_{2x})B_2$. Therefore, Fig. 3(c) does not have SSBs.

The formation of $(Mg_{1-x}Li_{2x})B_2$ is supported by many other observations. It is known that MgB_2 has a layered crystal structure where layers of boron are located between layers of magnesium [12,13], and Mg is ionized to be Mg^{2+} so that MgB_2 can be characterized by the ionic form $Mg^{2+}(B_2)^{2-}$ [14,15]. Furthermore, a previous study [8], based on the ^{11}B NMR analysis, has shown that the layered boron structure is not altered by ball milling of LiH + (1/2)MgB_2. Therefore, the Li^{+} ions in $(Mg_{1-x}Li_{2x})B_2$ must be located between the layered boron structures and replace Mg^{2+} ions to maintain the charge balance. Since Li ions are located between the layered boron structures, SSBs would occur in the ^{6}Li MAS spectrum (see Fig. 3(a) and (b)) because the layered boron structure resembles the graphite structure that would induce significant magnetic susceptibility due to delocalized electronic structures.

In addition, since the Li ions are close to the Mg ions in $(Mg_{1-x}Li_{2x})B_2$, the spin-lattice relaxation time of ^{6}Li would be reduced significantly because Mg is a known effective relaxation sink. Fig. 3(a) is successfully acquired using a recycle time of 0.2 s, unambiguously revealing that the T_1 of the Li-sites contributing to the signal is indeed very short. Finally, the formation of MgH_2 during ball milling of LiH + (1/2)MgB_2, as unveiled by the ^{25}Mg NMR analysis [8], also support the Li–Mg ion exchange model in forming $(Mg_{1-x}Li_{2x})B_2$ via the following reaction [8].

$$2LiH + MgB_2 \underset{\text{ball milling}}{\longrightarrow} (Mg_{1-x}Li_{2x})B_2 + xMgH_2 + (2-2x)LiH \quad (2)$$

Taking all of these evidence together, it can be safely concluded that ball milling of LiH + (1/2)MgB_2 has resulted in the formation of $(Mg_{1-x}Li_{2x})B_2$ with Li ions located between the layered boron structures and close to Mg ions.

Before concluding, it should be pointed out that the present NMR analysis using ^{1}H–^{6}Li cross polarization has unequivocally identified the peak position of the ^{6}Li sites in bulk LiH at 0 ppm. Therefore, previous studies [8,10] have mistakenly assigned the 2.76 ppm peak to LiH. It is noted that the present assignment of the 0 ppm peak to LiH is consistent with the previous reports of the ^{6}Li NMR spectrum of LiH acquired at a magnetic field of 11.7 T [16] and the ^{7}Li NMR spectrum of LiH attained at 9.7 T [17] and 14.1 T [18]. Another important question that needs to be addressed is where the position of the chemical shift is for the Li ions inside $(Mg_{1-x}Li_{2x})B_2$. However, it is not possible to answer this question using Fig. 3 because of the chemical shift of the centerband peak in Fig. 3(a) and (b) ranging from about −5 to 5 ppm and the relatively poor signal-to-noise ratio in the CP spectrum of the sample (Fig. 3(c)). Nevertheless, by comparing the positions of the centerband peaks between SP (Fig. 3(a) and (b)) and CP (Fig. 3(c)) spectra, it may conclude that downfield shift takes place when the Li ions in LiH becomes the Li ions in $(Mg_{1-x}Li_{2x})B_2$.

4. Concluding remarks

The present study with the detailed ^{1}H–^{6}Li cross polarization NMR analysis has unambiguously revealed that the ^{6}Li sites in LiH have the longest relaxation time, whereas the ^{6}Li sites in Li_2O have

the shortest relaxation time with the relaxation time of the ^{6}Li sites in LiOH between these two extremes. The formation of a ternary compound, $(Mg_{1-x}Li_{2x})B_2$, during ball milling of $LiH+(1/2)MgB_2$ at room temperature is confirmed by the present study. The ^{6}Li sites in $(Mg_{1-x}Li_{2x})B_2$ exhibit SSBs, whereas the ^{6}Li sites in LiH do not. The SSBs and the very short spin-lattice relaxation time manifested by the ^{6}Li sites in $(Mg_{1-x}Li_{2x})B_2$ indicate that the Li ions in $(Mg_{1-x}Li_{2x})B_2$ are located between the layered boron structures and close to Mg ions. The formation of $(Mg_{1-x}Li_{2x})B_2$ during ball milling of $LiH+(1/2)MgB_2$ provides a rational explanation on the previous observation that the $LiH+(1/2)MgB_2$ mixture ball-milled effectively has a greatly enhanced hydriding kinetics at temperatures below the melting point of $LiBH_4$ because the formation of $LiBH_4$ in the hydriding reaction requires the removal of Mg ions from MgB_2 in conjunction of the simultaneous insertion of Li and H ions.

Acknowledgements

The stimulating discussion with Dr. John Vajo at HRL Laboratories and Dr. Son-Jong Hwang at California Institute of Technology regarding the assignment of ^{6}Li peaks is greatly appreciated. This research was sponsored by the U.S. Department of Energy (DOE) under the contract number DE-FC36-05GO15008 with Dr. Ned T. Stetson as the Technology Manager. The NMR experiments were performed in the Environmental Molecular Sciences Laboratory, a national scientific user facility sponsored by the DOE Office of Biological and Environmental Research, and located at the Pacific Northwest National Laboratory, USA.

References

[1] J.J. Vajo, S.L. Skeith, F. Mertens, J. Phys. Chem. B 109 (2005) 3719–3722.
[2] X.B. Yu, D.M. Grant, G.S. Walker, Chem. Commun. (2006) 3906–3908.
[3] F.E. Pinkerton, M.S. Meyer, G.P. Meisner, M.P. Balogh, J.J. Vajo, J. Phys. Chem. C 111 (2007) 12881–12885.
[4] T. Nakagawa, T. Ichikawa, N. Hanada, Y. Kojima, H. Fujii, J. Alloys Compd. 446–447 (2007) 306–309.
[5] G.S. Walker, D.M. Grant, T.C. Price, X.B. Yu, V. Legrand, J. Power Sources 194 (2009) 1128–1134.
[6] J. Yang, A. Sudik, C. Wolverton, J. Phys. Chem. C 111 (2007) 19134–19140.
[7] X. Wan, T. Markmaitree, W. Osborn, L. Shaw, J. Phys. Chem. C 112 (2008) 18232–18243.
[8] J.Z. Hu, J.H. Kwak, Z. Yang, X. Wan, L. Shaw, Appl. Phys. Lett. 94 (2009) 141905.
[9] Z.-G. Yang, L. Shaw, Nanostruct. Mater. 7 (1996) 873–886.
[10] J.Z. Hu, J.H. Kwak, Z.G. Yang, W. Osborn, T. Markmaitree, L. Shaw, J. Power Sources 182 (2008) 278–283.
[11] A. Ortiz, W. Osborn, T. Markmaitree, L. Shaw, J. Alloys Compd. 454 (2008) 297–305.
[12] G. Barkhordarian, T.R. Jensen, S. Doppiu, U. Bsenberg, A. Borgschulte, R. Gremaud, Y. Cerenius, M. Dornheim, T. Klassen, R. Bormann, J. Phys. Chem. C 112 (2008) 2743–2749.
[13] E.D. Jemmis, E.G. Jayasree, Acc. Chem. Res. 36 (2003) 816–824.
[14] J.M. An, W.E. Pickett, Phys. Rev. Lett. 86 (2001) 4366–4369.
[15] J. Kortus, I.I. Mazin, K.D. Belashchenko, V.P. Antropov, L.L. Boyer, Phys. Rev. Lett. 86 (2001) 4366–4369.
[16] J. Lu, Z.Z. Fang, H.Y. Sohn, R.C. Bowman, S.-J. Hwang, J. Phys. Chem. C 111 (2007) 16686–16692.
[17] Z. Xiong, G. Wu, J. Hu, Y. Liu, P. Chen, W. Luo, J. Wang, Adv. Funct. Mater. 17 (2007) 1137–1142.
[18] O. Dolotko, H. Zhang, O. Ugurlu, J.W. Wiench, M. Pruski, L.S. Chumbley, V. Pecharsky, Acta Mater. 55 (2007) 3121–3130.